DETECTION OF WATER-BODY BOUNDARIES FROM SENTINEL-2 IMAGERY FOR FLOODPLAIN LAKES

[1]Azura Ulfa, [2]Fajar Bahari Kusuma, [3]A. A. Md. Ananda Putra Suardana, [1]Wikanti Asriningrum, [4]Andi Ibrahim, [5]Lintang Nur Fadlillah

[1]Research Center for Remote Sensing, National Research and Innovation Agency (BRIN) , Indonesia
[2]Center for Data and Information, National Research and Innovation Agency (BRIN) , Indonesia
[3]Research Center for Oceanography, National Research and Innovation Agency (BRIN), Indonesia
[4]Faculty of Geo-Information and Earth Observation, University of Twente, Enschede, The Netherlands
[5]Department Environmental Geography, Faculty of Geography, Universitas Gadjah Mada, Indonesia
e-mail: azur001@brin.go.id

Received: 30.12.2022; Revised: 31.12.2022; Approved: 01.01.2023

Abstract. The impact of climate and human interaction has resulted in environmental degradation. Consistent observations of lakes in Indonesia are quite limited, especially for flood-exposure lake types. Satellite imagery data improves the ability to monitor water bodies of different scales and the efficiency of generating lake boundary information. This research aims to detect the boundaries of flood-exposure type lake water bodies from the detection model and calculate its accuracy in Semayang Melintang Lake using Sentinel-2 imagery data. The characteristics of water, soil, and vegetation objects were investigated based on the spectral values of the composite image bands from the Optimum Index Factor (OIF) calculation, to support the lake water body boundary detection model. The Object-Based Image Analysis (OBIA) method is used for water and non-water classification, by applying the machine learning algorithms random forest (RF), support vector machine (SVM), and decision tree (DT). Model validation was conducted by comparing spectral profiles and lake water body boundary model results. The accuracy test used the confusion matrix method and resulted in the highest accuracy value in the SVM algorithm with an Overall Accuracy of 95% and a kappa coefficient of 0.9. Based on the detection model, the area of Lake Semayang Melintang in 2021 is 23392.30 ha. This model can be used to estimate changes in the area of the flood-exposure lake consistently. Information on the boundaries of lake water bodies is needed to control the decline in the capacity and inundation area of flood-exposure lakes for management and monitoring plans.

Keywords: *Lake, floodplain, remote sensing, OBIA, water bodies*

1 INTRODUCTION

Terrestrial water bodies make up only about 2.5-2.75% of the total amount of water on Earth. The water cycle plays an important role in the balance of processes on Earth (Berghuijs et al., 2021). Human activities increase the pressure on water and land (Faksomboon, 2022).

Water resources are becoming increasingly important for human consumption due to population growth and economic activities. However, environmental degradation has resulted in a decline in quantity and quality (Regasa et al., 2021) and extreme climatic conditions threaten the ecological functions of water bodies (Adrian et al., 2009).

The size, shape, and freshwater distribution of lakes provide challenges in manual watershed assessment, namely in terms of labor, time, cost (Buma et al., 2018), accuracy, and efficiency in extracting water bodies (Kang et al., 2021). Remote sensing technology can be an effective solution to assessing the quantity and quality indicators of lake water bodies (J. Li et al., 2022); (Julzarika et al., 2019).

The utilization of remote sensing satellite images for water body detection is highly recommended for large areas, difficult to reach, and short time (Kang et al., 2021); (Pekel et al., 2016). Mapping the spatial distribution of water bodies has proven to be cost-effective as well as an evolving and sustainable processing method (Craglia et al., 2012); (Trisakti et

al., 2014). Survey and mapping of water bodies are essential for water resource utilization, flood monitoring, and environmental protection (Kang et al., 2021).

Data sources to generate water body information can be extracted from optical remote sensing and microwave radar remote sensing (Armi & Antom, 2021); (Liao & Wen, 2020); (Chulafak et al., 2021). Conventional water body extraction methods can be categorized into threshold methods and machine learning methods. Threshold methods include single-band and multi-band methods. Among these methods, there are water body index and segmentation methods, including various water body indices NDWI, NDWI3, MNDWI, and even NDVI (McFeeters, 1996).

The current development is the use of machine learning methods to detect water bodies from remote sensing data by analyzing training samples which are divided into supervised and unsupervised methods, such as Support Vector Machine (SVM) (Liu et al., 2020); (Otukei & Blaschke, 2010), Decision Tree (DT) (Chen et al., 2022); (Setiawan et al., 2022), Random Forest (RF) (Purwanto et al., 2022), and even deep learning (K. Li et al., 2022) have been applied to detect lake water body boundaries.

While water bodies are distinguished based on the spectral characteristics of vegetation and soil objects, other methods can combine multiple characteristics to classify and identify these objects. The accuracy of each algorithm will be different. Comparison of multiple algorithms will produce the best accuracy value (Otukei & Blaschke, 2010).

The area of the water body in the lake will impact the determination of the boundary. There are no problems in determining the boundaries of lake edges in tectonic, volcanic, dam, and tecto-volcanic types. Problems occur in flood-exposure-type lakes due to the complexity of determining the fixed boundaries of their surface area (Julzarika et al., 2019).

A flood-exposure lake is a natural water reservoir that is part of a river whose water level is directly affected by the river's water level (PUPR, 2015). The Mahakam cascade is a group of lakes with 3 large lakes in it, including Lake Jempang, Semayang, and Melintang (Muchlis et al., 2021). The cascade lakes have a complex hydrological system, during floods these three lakes merge with the Mahakam River, but during the dry season the water recedes, and the lake banks become dry land or form deep and waterlogged furrows. Fluctuations in the water level of the Mahakam Cascade lakes are very high ranging from 1-12 m (Anwar et al., 2022).

Semayang Melintang Lake is located in Kutai Kartanegara, East Kalimantan. This lake is one of the 15 national priority lakes that is currently categorized as a critical lake. Determining the water body boundaries of flood-exposure type lakes is quite difficult due to its complexity (Julzarika et al., 2019), so a water body boundary detection model with good accuracy is needed to support monitoring efforts for flood-exposure type lakes in Indonesia, especially Semayang Melintang Lake.

The study of in the Mahakam Cascade produced water boundaries in flood inundation using ALOS PALSAR radar backscatter (Hidayat et al., 2012). (Julzarika et al., 2019) determined the boundaries of the lake edge of flood exposure with the harmonic modeling method using radar data on Sentinel 1 imagery on Semayang, Melintang, and Jempang Lakes.

This study aims to detect the boundary of a flood-exposed type lake water body from a detection model using the object-based image analysis method and calculate its accuracy from Sentinel-2 satellite imagery. The spectral profileprofile is compared with the lake water body boundary model for validation and accuracy test. This research is to support the management of lake water resources based on remote sensing imagery.

2 MATERIALS AND METHODOLOGY

2.1 Location and Data

The study site is located in Semayang Melintang Lake, Kutai Kartanegara, East Kalimantan. Semayang Melintang Lake is called the Middle Mahakam Area (MMA), which is part of the Mahakam Cascade of lake complexes in the Mahakam River basin with low relief and 40 shallow lakes on either side (Hidayat et al., 2012). This lake regulates the discharge in the downstream area of the Mahakam, which functions as a buffer, storing water when the discharge is high and draining water when the flow is low (Hidayat et al., 2011).

It is an inundated freshwater ecosystem and includes eutrophic-type floodplain waters with muddy and sandy floors. Eutrophic lakes are lakes that contain a lot of nutrients, especially nitrate and phosphorus, which cause the growth of algae and aquatic plants to increase

Semayang Lake has an area of 13,000 ha with an average depth of 3.5 m, while Melintang Lake has an area of 11,000 ha with an average depth of 2 m (Julzarika et al., 2019). The MMA is surrounded by peatlands as part of the kutai lowlands. The soil type is clay which can store water. Land cover conditions in the Mahakam Cascade Lake include water bodies 19,304 ha, swamps 36,265 ha, shrubs 4,139 ha, and settlements 135 ha (Direktorat Pengendalian Kerusakan Perairan Darat., 2019).

The average daily temperature around Semayang Melintang Lake is 24-29 °C, humidity is 73-99%, and rainfall averages 2300 mm/year. Water level fluctuations are extreme at 1-12 m. The Mahakam Cascade Lake recorded the highest flood reaching 14.54 m (Anwar et al., 2022).

The study site can be seen in Figure 2-1.

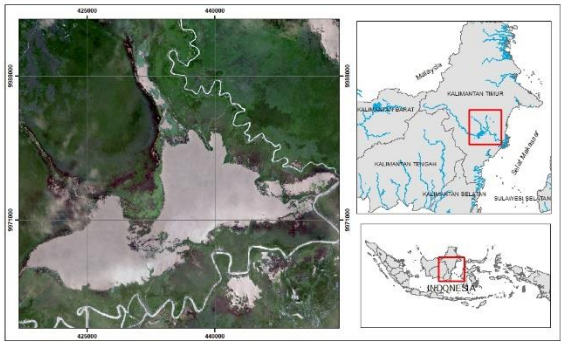

Figure. 2-1: Study site Semayang Melintang Lake, East Kalimantan

The data used in this study is the Sentinel-2 Level 2 satellite image recorded on October 12, 2021. This data was obtained from the Research Center for Remote Sensing, BRIN as the official institution in image data acquisition in Indonesia.

2.2 Optimum Index Factor (OIF)

The Optimum Index Factor (OIF) calculation is performed to find the right combination of channels to visualize significant differences between water and non-water. The OIF results in one selected channel composite that will be used to extract the observed object and used for visual detection of water bodies.

The OIF calculation process is conducted using the matrix correlation method with the following equation 2-1:

$$OIF = \frac{\sum_{k=1}^{3} S_k}{\sum_{j=1}^{3} Abs\,(r_j)} \quad \text{.....(2-1)}$$

Description :

S_k : Standard deviation of spectral values in the channel

Abs (r_j) : The absolute value of the correlation coefficient between each two of the three channels

(Chavez et al., 1982)

2.3. Transect line

Drawing transect lines aims to obtain spectral values that represent water and non-water objects. The boundary of the lake water body can be seen on the spectral profile through changes in the graph pattern in each band. Spectral profiles are used for model validation and help in testing the accuracy of the flood exposure lake water body

boundary detection model. Transect lines were taken twice vertically and once horizontally. secara horizontal.

2.4. Segmentation

There are two processing stages in the object-based image analysis (OBIA) method, namely segmentation, and classification. The segmentation process is done to build objects/segments from pixels into the same object/segment. The method used is multiresolution segmentation with the following equation (Baatz & Schäpe, 2000) berikut:

$S_f = w_{colour} \times hz_{colour} + (1 - w_{colour} \times h_{shape})$.....(2-2)

Description :
S_f : segmentation function
w_{colour} : color parameter weight
h_{colour} : color parameter
h_{shape} : shape parameter weight
w_{shape} : shape parameter

2.5. Classification

The classification technique performed to detect lake water bodies uses object-based classification. The OBIA method is developed with the process of segmentation and object analysis. The classification process is based on spatial, spectral, and temporal scale characteristics, resulting in image objects or segments that are then used for classification (Purwanto et al., 2022); (Mastu et al., 2018).

Classification aims to group segmented image objects into various types of classes into one commonality with a certain system. The classes used in lake water body boundary detection are water and non-water.

The classification method is carried out by applying several machine learning algorithms, including random forest (RF), support vector machine (SVM), and decision tree (DT). The classification results of each algorithm will be compared based on the accuracy value. The formula of each classification algorithm used is as follows:

Random forests (Phan et al., 2020); (Breiman, 2001):

$forest = \{h(x, \theta_k), k = 1, \dots\}$..... (2-3)

Description :
h : *Hypothesis* atau *classifier* (*decision tree*)
x : *Input vector*
θ_k: *Independent and identically distributed* (IID) *random vectors*

$\hat{C}_{rf} = majority\ vote\ \{\hat{C}_n(x)\}_n^N = 1$ ..... (2-4)

Description :
$\hat{C}_{rf}$: Random forest result class. The hat operator in $\hat{C}$ indicates that the class is an estimated class
x : *Input vector*
$\hat{C}_n$: Prediction class of the nth tree in a random forestt

SVM (Tzotsos, 2006):

$f(x) = \sum_{i \in S} \lambda_i y_i K(x_i x) + w_0$ ..... (2-5)

Description : K is a kernel function, yi and xi represent training samples, ⋋i are Lagrange multipliers, part of the training sample corresponding to a non-zero Lagrange multiplier, and ω_0 is a hyperplane parameter

DT (Bradski & Kaehler, 2008):

$Gini\ impurity: i(N) = \sum_{j \neq i} P(\omega_i) P(\omega_j)$ ..... (2-6)

Keterangan: This method uses the notationP(ωj) to denote the fraction of patterns at node N that are in class ωj.

2.6. Accuracy Test

The accuracy test uses the confusion matrix method. The confusion matrix is a table used to measure the relationship between two categorical variables where the table summarizes the joint frequency of observations in each variable category(Dong et al., 2022). The equation used for the accuracy test is as follows:

$overall = (aA+bB)/N$ .....(2-7)
$produser = aA/\sum A$ ..... (2-8)
$user = aA/\sum a$ ..... (2-9)
$kappa = \frac{\frac{\sum a \times \sum A}{N} + \frac{\sum b \times \sum B}{N}}{N}$ .....(2-10)

The research flowchart can be seen in Figure 2-2.

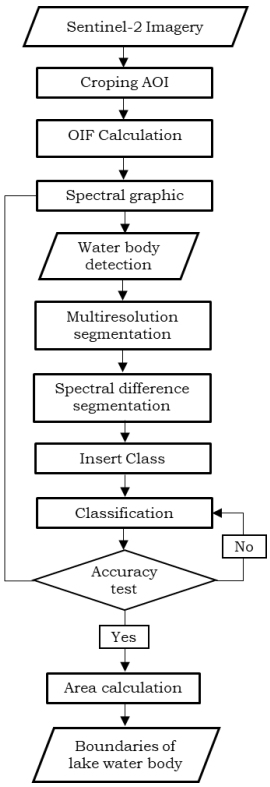

Figure. 2-2: Research flow chart

3 RESULTS AND DISCUSSION

3.1. Water Body Detection

Optimun Factor Index (OIF)

The focus of this research is Lake Semayang Melintang, Kutai Kartanegara, East Kalimantan. This lake is a type of Floodplain Lake. The process of detecting water bodies is done visually and digitally. Visually, the OIF calculation is performed and the transect line is drawn. The results of this process are used to validate the detection model and assist in testing the accuracy of the model.

OIF calculations are performed to determine the best combination of composite bands in detecting water bodies and non-water bodies for determining the boundaries of water bodies in floodplain lake types.

The data used in the OIF calculations is sentinel-2A imagery recorded on October 12, 2021. The bands used are blue, green, red, red edge, NIR, and SWIR. OIF produces the best composite by calculating the standard deviation and correlation coefficient of the band combinations used (Purwanto & Setiawan, 2019).

The results showed that the composite combination 2(blue), 4(red), 8(NIR) had the highest OIF value for Sentinel-2A imagery. Interpretation of water bodies can be done effectively by using RGB 248 composite images.

The OIF value on RGB 248 is 9415.41, with a total standard deviation of 1725.32. Table 3-1 presents OIF values and ratings for Sentinel-2 images.

Table 3-1: OIF Value and Citra Sentinel-2 Combined Rating

No	Combination	Total Sd	OIF	Rating
1	248	1725.32	9415.41	Rating 1
2	348	1677.88	5496.11	Rating 2
3	238	1652.35	4854.36	Rating 3
4	4810	1526.25	4752.9	Rating 4
5	2810	1500.72	4259.25	Rating 5
6	458	1619.81	3619.61	Rating 6

Based on the OIF value and the combined Sentinel-2 imagery rating, the highest standard deviation will result in the highest OIF value. The results of the study (Purwanto & Setiawan, 2019), show that the channel combination that produces the highest OIF value will have a high standard deviation value and a low correlation coefficient, and vice versa.

This is in accordance with research(Debdib, 2013) which explains that the higher the total standard deviation of the 3 bands used indicates the more information is generated, while the smaller the total correlation coefficient between the 2 bands indicates the less duplication is generated.

Figure 3-1 shows the composite band 248 combination which has the highest OIF value from the Sentinel-2A image so that it provides the best and most informative view compared to other combinations. RGB 248 provides a good display in distinguishing water bodies and non-water bodies. RGB 248 results show water bodies displayed in bright yellow and non-water bodies in dark blue.

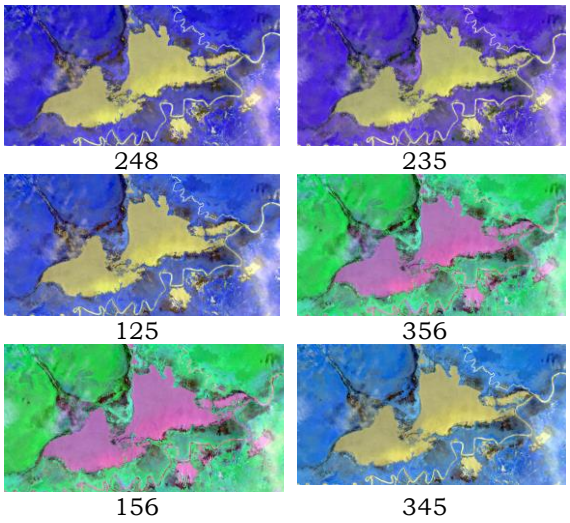

Figure. 3-1: Sentinel-2 Imagery OIF Calculation Channel Composite

Spectral profile

The spectral profile describes the characteristics of each band against objects that pass through it. Spectral profile are used for model validation and help test the accuracy of the water body boundary detection model.

The selected band is based on the results of the OIF calculation, namely RGB 2 (blue), 4 (red), 8(NIR). Transect 1 is drawn vertically from top to bottom and produces a spectral profile, where the blue line is band 2(blue), the green line is band 4(red), and the red line is band 8(NIR).

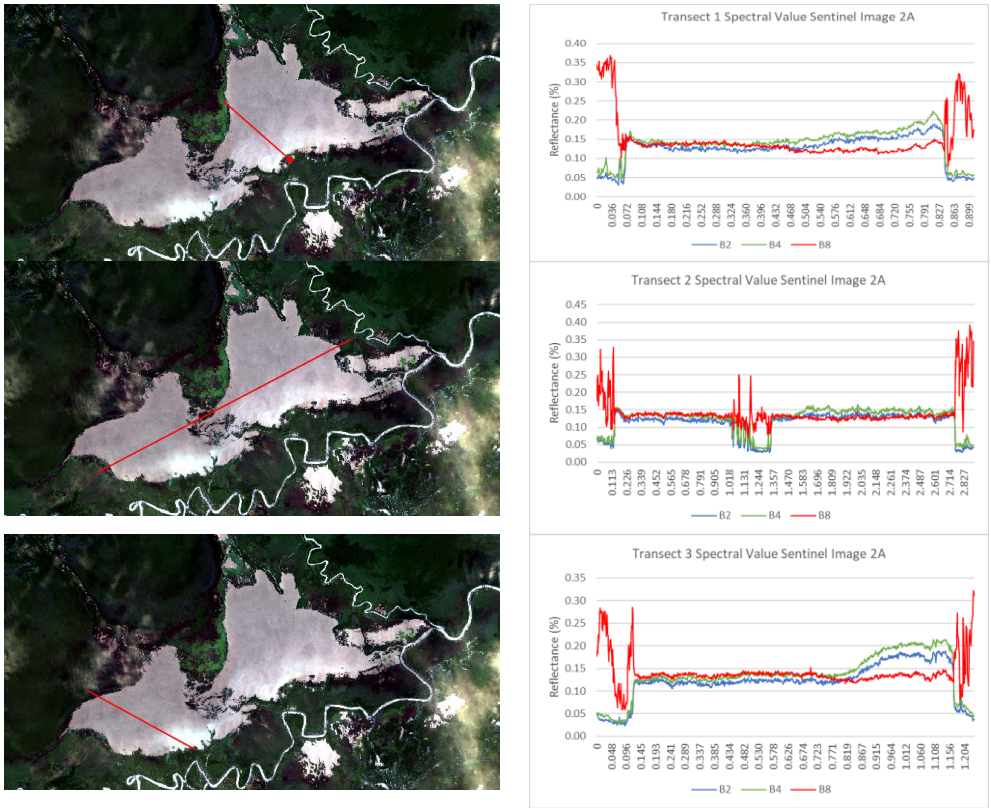

Figure 3-2: Sentinel-2A RGB 248 Image Spectral Profile

Based on Figure 2-3, the boundary between water and non-water can be seen very clearly through the graphic pattern. When it encounters a water object, the spectral value in bands 2 (blue) and 4 (red) will increase, while in band 8 (NIR) it will decrease. These results are also supported by research (Asriningrum et al., 2022), passing through water objects in the lagoon, the spectral value in the NIR band is very small when compared to the blue and green bands.

3.2. Image Classification and Water Body Boundaries of Lakes

Segmentation

The segmentation process produces segments based on pixel values and objects in the image. The segmentation process is carried out in 2 stages. The composite image used is RGB 248. The segmentation process greatly influences the classification results, so the appropriate segmentation parameters are needed. This statement is supported by research (Purwanto et al., 2022).

The level 1 segmentation process uses a scale parameter with a value of 100, shape with a value of 0.2 and compactness with a value of 0.7. The results of the first segmentation can be seen in Figure 3-3. While the level 2 segmentation process is based on pixel values and objects from the image with the parameter used is the maximum spectral difference (100) (Figure 3-4).

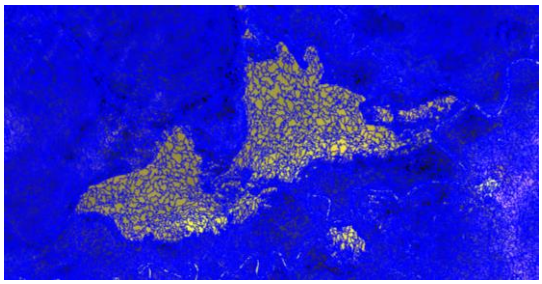

Figure 3-3 : Level 1 Segmentation

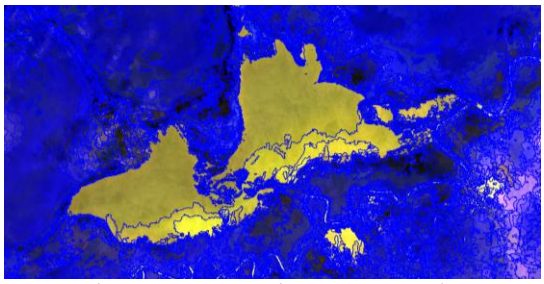

Figure 3-4 : Level 2 Segmentation

Multilevel segmentation produces segments that are more general and produce better shape objects according to the pixel values in the image. Level 1 produces 15.493 segments, while level 2 produces 8.440 segments.

Image Classification

The classification process produces classes of water and non-water objects. Sample training was taken for each class. The Object Based Image Analysis method is applied with machine learning random forest algorithms, support vector machines, and decision trees.

Classification of water and non-water produces the boundaries of lake water bodies. Next, a calculation of the area of Semayang Melintang lake is carried out for image recording in 2021. The last step is to calculate the accuracy of the results of the lake water body boundary detection modeling.

Based on the classification results, lake information is generated as shown in Figure 3-5.

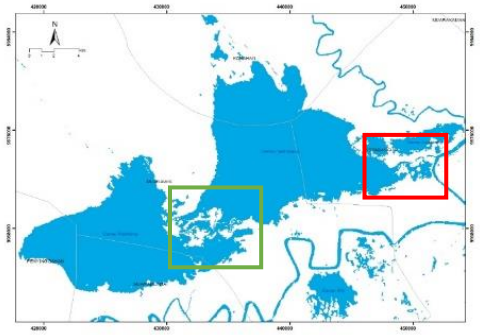

RF

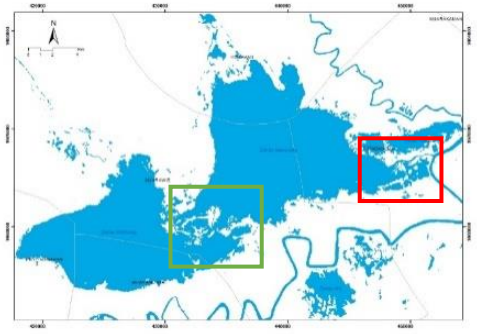

SVM

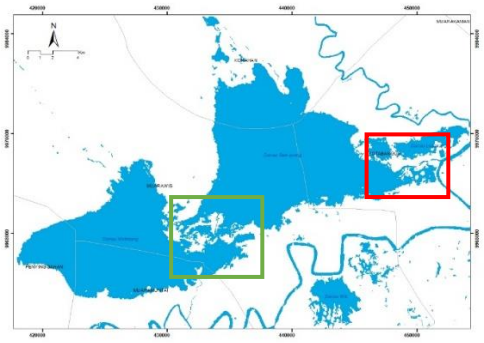

DT

Figure 3-5: Results of Lake Detection the Object-Based Classification Process (Green box is settlement between two lakes; Red box ismodel differences at the outlet of the lake)

Based on the classification results, the blue color indicates the detected water body from the image. While the white color is non-water including vegetation and soil objects. The detected water bodies include lakes, main rivers, seasonal bodies, and inundations. Based on the classification results, the OBIA method with the application of machine learning algorithms can detect water bodies in images quite well. This detection model can be applied to other image recordings, in an effort to manage Lake Semayang Melintang.

The quite extreme fluctuations in Lake Semayang Melintang due to the influence of the seasons make it very difficult to determine the boundaries of the lake's water bodies. This statement is supported by research (Muh Fakhrudin, 2020), where the Mahakam Cascade Lake during the rainy season several lakes will merge with the Mahakam River, but during the dry season only deep grooves remain.

Figure 3-6: Community Settlements (Source : Dinas Pariwisata Kalimantan Timur, 2022

In extreme conditions, flooding during the rainy season can occur around the lake, submerging the settlements between Lake Semayang and Melintang, shown by the green box. This is in accordance with research (Anwar et al., 2022), where the Mahakam Cascade recorded the highest floods in 2007 reaching 15.54 m. The vulnerability of the people of Melintang Village to the Lake Melintang flood disaster is only 45% (moderate). Figure 3-6 shows the location of community settlements in the green box.

Water Body Boundaries

Figure 3-7 presents a subset of the extracted water bodies obtained from several locations on Sentinel-2 imagery from the test data. The first column shows the differences in the results of the detection of water body boundaries in each of the machine learning classification methods which are quite varied. Water bodies are detected in the SVM algorithm. While the DT and RF algorithms are not detected.

Based on the third and fourth columns, the SVM algorithm accurately describes isolated bodies of water, while RF and DT do not classify some objects in detail. Overall, the results of the water body boundaries detection model with the SVM algorithm provide quite detailed and good results. The SVM algorithm provides detailed and sensitive classification results for isolated water objects. The boundaries of settlement objects and sedimentary waters can be fairly well distinguished.

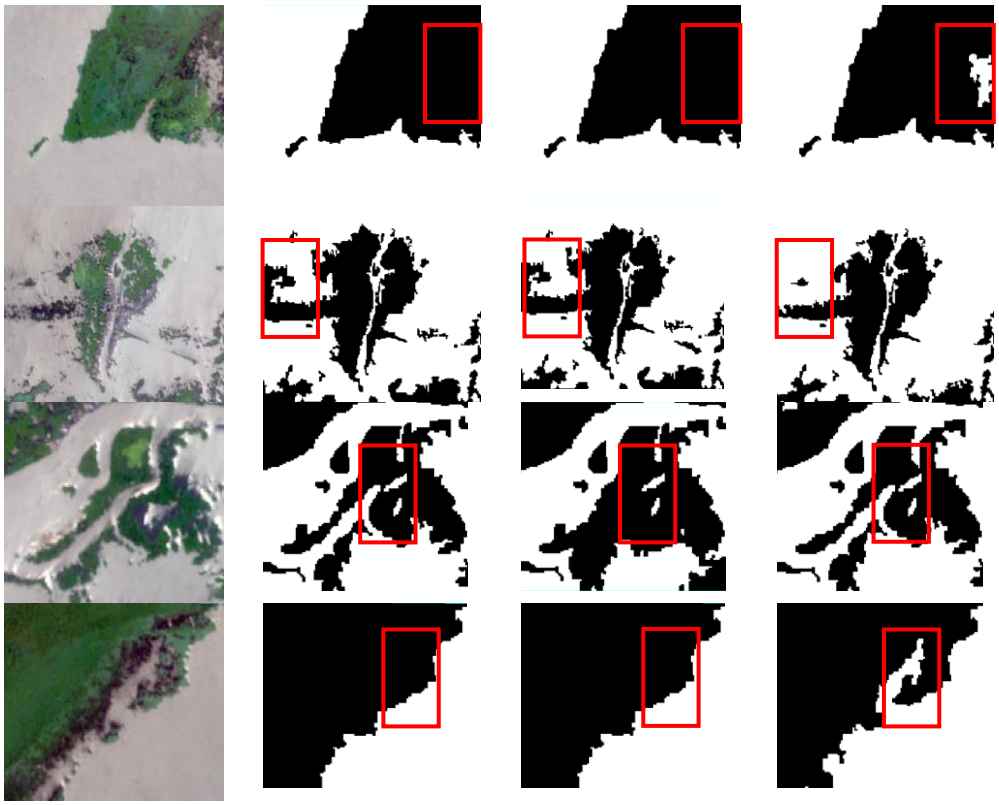

Figure 3-7: Comparison of Image and Results Water body boundaries at several locations

The Area of Lake Semayang Melintang

The results of processing the Sentinel-2 Image recorded on August 12, 2021, resulted in the area of Lake Semayang Melintang using several algorithms. The area results show that the distribution of water in Lake Semayang Melintang is quite wide.

Figure 3-8 The red lines show the results of the DT algorithm, the red lines show the RF results, and the green shows the SVM. The results of calculating the area of each algorithm are shown in Table 3-2.

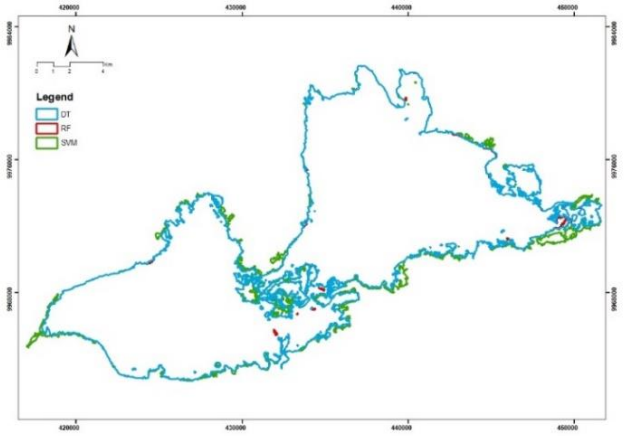

Figure 3-8: Semayang Melintang Lake Boundary from Citra Sentinel-2

There are wide differences of processing results. The area of Lake Semayang Melintang for the SVM algorithm is 23392.30 ha, while RF is 22477.61 ha, and DT is 22548.78 ha. The SVM algorithm produces the largest area of all the algorithms used.

Research conducted by (Julzarika et al., 2019) namely processing with Sentinel 1 and Landsat 8 image data in 2018, resulted in an area of Lake Semayang Melintang of 24901 ha and 24949. Meanwhile research conducted by (M Fakhrudin et al., 2004) producing an area of 16580 ha. TKPSDA WS Mahakam and the Ministry of PUPR recorded that the area of Lake Semayang Melintang in 2017 was 24,000 ha.

Based on the results of modeling and literature, there has been a change in area from 2004, 2017, 2018 and 2021. The trend of the area of Semayang Melintang Lake water bodies has increased until 2018, and decreased in 2021.

Table 3-2: Area of Lake Semayang Melintang on Several Algorithms

No	Data	Area (ha)	Area (km²)
1	SVM	23392.30	233.92
2	RF	22477.61	224.78
3	DT	22548.78	225.49

3.3. Accuracy and Validation of Water Body Detection

Model validation is done by comparing the results of the transect line drawing with the results of the model being carried out. The results of the spectral profile 1 show that the boundary value between water and non-water has a spectral value of 0.14%. Based on model validation, it appears that the model can detect lake water body boundaries well. Figure 3-9 shows the validation of the model on one of the transect lines in Lake Semayang.

Results of the Lake Water Body Detection Model

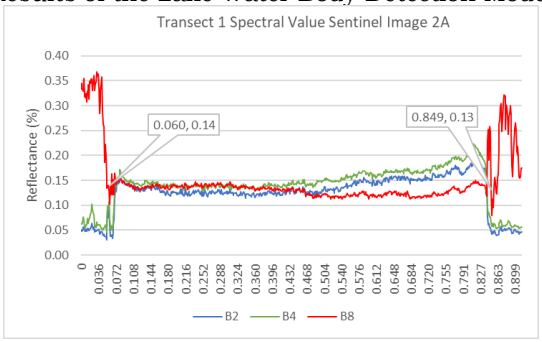

Transect Spectral profile 1

Figure 3-9: Validation of the result og the SVM method detection model

Evaluate the performance of several algorithms used to detect Lake Semayang Melintang water bodies by calculating producer, user, overall accuracy, and kappa coefficient accuracy. Sentinel-2 imagery recorded on August 12, imagery from Google Earth, and the spectral chart drawn from the transect line are used as a reference to assess the accuracy of the lake water body detection model. The accuracy calculation results for the SVM, RF, and DT algorithms can be seen in Tables 3-4, 3-5, and 3-6.

Comparison between pixels is performed to produce an error matrix. The error matrix produces producer and user accuracy values, overall accuracy, and the kappa coefficient. SVM has an overall accuracy of 95%, a kappa coefficient of 0.9, producer and user accuracy for water is 90% and non-water is 100%. The model can distinguish water very well. Based on the accuracy calculation results, the SVM algorithm gives the best results.

Tabel 3-3: SVM Accuracy Test Calculation Results

SVM					**Kappa: 0.9**
Classification		**Water**	**Non Water**	**Total**	**User**
	Water	20	0	20	100 %
	Non Water	2	18	20	90%
	Total	22	18	40	
	Producer	90%	100%		**95%**

Tabel 3-4: RF Accuracy Test Calculation Results

RF					**Kappa: 0.9**
Classification		**Water**	**Non Water**	**Total**	**User**
	Water	19	1	20	95%
	Non Water	1	19	20	95%
	Total	20	20	40	
	Producer	95%	95%		**95%**

Tabel 3-5: DT Accuracy Test Calculation Results

DT					**Kappa: 0.9**
Classification		**Water**	**Non Water**	**Total**	**User**
	Water	19	1	20	95%
	Non Water	1	19	20	95%
	Total	20	20	40	
	Producer	95%	95%		**95%**

DT and RF have an overall accuracy of 95% and a kappa coefficient of 0.9. Producer and user values for water are 95% and non-water are 95%. Based on the calculation results, the accuracy values of the 3 algorithms are relatively stable and all algorithms can detect bodies of water with an overall accuracy greater than 94%. The user and producer accuracy values in the SVM algorithm are higher than other algorithms.

This result is also corroborated by research (J. Li et al., 2022), water bodies can be detected properly, when compared to the water index, the SVM algorithm provides greater accuracy, namely OA: 97% and Kappa: 0.95. While research (Purwanto et al., 2022) detect benthic habitat objects and produce an accuracy value for SVM of 75%, research (Liu et al., 2020) detecting bodies of water produces an accuracy value of 98% in the SVM algorithm. When compared to the water index, detection using the OBIA algorithm SVM method provides more detailed and accurate results.

4 CONCLUSIONS

Based on the results obtained, it can be concluded that goba detection based on the results of OIF calculations produces a composite RGB248 image (which can visually detect lake water bodies well. Based on the water body boundaries detection model, the SVM algorithm has good results (OA: 95%, kappa : 0.9, area 23392.30 ha. The SVM algorithm provides detailed and sensitive classification results for isolated water objects. The boundaries of settlement objects and sedimentary waters can be quite well distinguished. Model validation from spectral profile results in lake water body boundaries in the range of values 0.13-0.14%.Based on a comparison of research results, the trend of the area of Lake Semayang Melintang increased from 2004-2018 and decreased in 2021 (model results).This model can be used to estimate changes in the area of Floodplain lakes consistently.

ACKNOWLEDGEMENTS

This research was funded by the Earth and Maritime Research Organization House, the National Research and Innovation Agency (BRIN). The authors thank the Remote Sensing Research Center for their assistance. We also appreciate the reviewers of this paper for constructive comments

REFERENCES

Adrian, R., O'Reilly, C. M., Zagarese, H., Baines, S. B., Hessen, D. O., Keller, W., Livingstone, D. M., Sommaruga, R., Straile, D., Van Donk, E., Weyhenmeyer, G. A., & Winder, M. (2009). Lakes as sentinels of climate change. Limnology and Oceanography, 54(6 PART 2), 2283–2297.https://doi.org/10.4319/lo.2009.54.6_part_2.2283

Anwar, Y., Maulana, M. F., Goma, E. I., Iya'Setyasih, & Wibowo, Y. A. (2022). Ketahanan Masyarakat Desa Melintang Terhadap Bencana Banjir Danau Melintang. Jurnal Pendidikan Geografi Undiksha, 10(2), 209–223. https://ejournal.undiksha.ac.id/index.php/JJPG

Armi, F. I., & Antom, Y. (2021). Konstruksi Spasial Genangan Banjir Menggunakan Citra Satelit Sentinel 1 Synthetic Aperture Radar (Sar) Di Propinsi Kalimantan Selatan. Jurnal Spasial, 5, 54–62. http://ejournal.stkip-pgri-sumbar.ac.id/

Asriningrum, W., Ulfa, A., Aziz, K., Setiawan, K. T., & Pangastuti, D. (2022). Platform Reef Lagoon Detection From Sentinel-2 In Panggang Island And Semakdaun Island. International Journal of Remote Sensing and Earth Sciences.

Baatz, M., & Schäpe, A. (2000). Multiresolution segmentation: an optimization approach for high quality multi-scale image segmentation. XII Angewandte Geographische Informations Verarbeitung, Wichmann- Verlag, Heidelberg.

Berghuijs, W. R., Luijendijk, E., Moeck, C., Van Der Velde, Y., & Allen, S. T. (2021). Global Recharge observations indicate strengthened groundwater connection to surface fluxes. Geophysical Research Letters, 1–9. https://doi.org/10.1029/2022GL099010

Bradski, G., & Kaehler, A. (2008). Learning opencv: Computer vision with the opencv library. O'Reilly Media.

Breiman, L. (2001). Random Forest. Machine Learning, 45, 5–32. https://doi.org/10.1007/978-3-030-62008-0_35

Buma, W. G., Lee, S. Il, & Seo, J. Y. (2018). Recent surface water extent of lake Chad from multispectral sensors and GRACE. Sensors, 18(7). https://doi.org/10.3390/s18072082

Chavez, P. S., Berlin, G. L., & Sowers, L. B. (1982). Statistical Method for Selecting Landsat Mss Ratios. Journal of Applied Photographic Engineering, 8(1), 23–30.

Chen, C., Chen, H., Liang, J., Huang, W., Xu, W., Li, B., & Wang, J. (2022). Extraction of Water Body Information from Remote Sensing Imagery While Considering Greenness and Wetness Based on Tasseled Cap Transformation. Remote Sensing, 14(13).https://doi.org/10.3390/rs14133001

Chulafak, G. A., Kushardono, D., & Yulianto, F. (2021). Utilization of Multi-Temporal Sentinel-1 Satellite Imagery for Detecting Aquatic Vegetation Change in Lake Rawapening, Central Java, Indonesia. Papers in Applied Geography, 7(3), 316–330. https://doi.org/10.1080/23754931.2021.1890193

Craglia, M., de Bie, K., Jackson, D., Pesaresi, M., Remetey-Fülöpp, G., Wang, C., Annoni, A., Bian, L., Campbell, F., Ehlers, M., van Genderen, J., Goodchild, M., Guo, H., Lewis, A., Simpson, R., Skidmore, A., & Woodgate, P. (2012). Digital Earth 2020: Towards the vision for the next decade. International Journal of Digital Earth, 5(1), 4–21. https://doi.org/10.1080/17538947.2011.638500

Debdib, B. (2013). Optimum Index Factor (OIF) for Landsat Data : a Case Study

on Barasat Town ,. International Journal of Remote Sensing & Geoscience (IJRSG), 2(5), 11–17.

Direktorat Pengendalian Kerusakan Perairan Darat. (2019). Rencana Pengelolaan Danau Kaskade Mahakam, Kementrian Lingkungan Hidup dan Kehutanan.

Dong, Y., Fan, L., Zhao, J., Huang, S., Geiß, C., Wang, L., & Taubenböck, H. (2022). Mapping of small water bodies with integrated spatial information for time series images of optical remote sensing. Journal of Hydrology, 614(July). https://doi.org/10.1016/j.jhydrol.2022.128580

Fakhrudin, M, Apip, & I, R. (2004). Kajian Water Balance Sebagai Dasar Pengelolaan Danau Semayang – Melintang Kutai Kartanegara Kaltim. Perubahan Iklim Dan Lingkungan Di Indonesia, 353–360.

Fakhrudin, Muh. (2020). Karakteristik Hidrologi Sebagai Dasar Pengelolaan Danau Cascade Mahakam. Prosiding Pertemuan Ilmiah Tahunan Ke IV Masyarakat Limnologi Indonesia : Penguatan Peran Limnologi Dalam Pemulihan Fungsi Ekosistem Perairan Darat, Tahun 2020, 365.

Faksomboon, B. (2022). Development of a Hydrodynamic Model for Regulating Water Drainage of Reservoir and Water Resources Management , Lamtakong Watershed of. Journal of Environmental Design and Planning, 21, 1–19.

Hidayat, H., Hoekman, D. H., Vissers, M. A. M., & Hoitink, A. J. F. (2012). Flood occurrence mapping of the middle Mahakam lowland area using satellite radar. Hydrology and Earth System Sciences, 16(7), 1805–1816. https://doi.org/10.5194/hess-16-1805-2012

Hidayat, H., Vermeulen, B., Sassi, M. G., F. Torfs, P. J. J., & Hoitink, A. J. F. (2011). Discharge estimation in a backwater affected meandering river. Hydrology and Earth System Sciences, 15(8), 2717–2728. https://doi.org/10.5194/hess-15-2717-2011

Julzarika, A., Dewi, E. K., & Subehi, L. (2019). Penentuan Batas Tepi Danau Paparan Banjir Secara Hitung Perataan Kuadrat Terkecil Dengan Multidata Pengindraan Jauh. Limnotek : Perairan Darat Tropis Di Indonesia, 26(2), 103–117. https://doi.org/10.14203/limnotek.v26i2.243

Kang, J., Guan, H., Peng, D., & Chen, Z. (2021). Multi-scale context extractor network for water-body extraction from high-resolution optical remotely sensed images. International Journal of Applied Earth Observation and Geoinformation, 103, 102499. https://doi.org/10.1016/j.jag.2021.102499

Li, J., Ma, R., Cao, Z., Xue, K., Xiong, J., Hu, M., & Feng, X. (2022). Satellite Detection of Surface Water Extent: A Review of Methodology. Water, 14(7), 1–18. https://doi.org/10.3390/w14071148

Li, K., Wang, J., Cheng, W., Wang, Y., Zhou, Y., & Altansukh, O. (2022). Deep learning empowers the Google Earth Engine for automated water extraction in the Lake Baikal Basin. International Journal of Applied Earth Observation and Geoinformation, 112(July), 102928. https://doi.org/10.1016/j.jag.2022.102928

Liao, H. Y., & Wen, T. H. (2020). Extracting urban water bodies from high-resolution radar images: Measuring the urban surface morphology to control for radar's double-bounce effect. International Journal of Applied Earth Observation and Geoinformation, 85(June 2019), 102003.https://doi.org/10.1016/j.jag.2019.102003

Liu, Q., Huang, C., Shi, Z., & Zhang, S. (2020). Probabilistic river water

mapping from Landsat-8 using the support vector machine method. Remote Sensing, 12(9). https://doi.org/10.3390/RS12091374

Mastu, L. O. K., Nababan, B., & Panjaitan, J. P. (2018). Pemetaan Habitat Bentik Berbasis Objek Menggunakan Citra Sentinel-2 Di Perairan Pulau Wangi-Wangi Kabupaten Wakatobi. Jurnal Ilmu Dan Teknologi Kelautan Tropis, 10(2), 381–396. https://doi.org/10.29244/jitkt.v10i2.21039

McFeeters, S. K. (1996). The use of the Normalized Difference Water Index (NDWI) in the delineation of open water features. International Journal of Remote Sensing, 17(7), 1425–1432. https://doi.org/10.1080/01431169608948714

Muchlis, A., Montarcih, L., Bisri, M., & Sholichin, M. (2021). Analisa debit banjir danau kaskade Mahakam. Pertemuan Ilmiah Tahunan HATHI Ke-38, 199–208.

Otukei, J. R., & Blaschke, T. (2010). Land cover change assessment using decision trees, support vector machines and maximum likelihood classification algorithms. International Journal of Applied Earth Observation and Geoinformation, 12(SUPPL. 1), 27–31.https://doi.org/10.1016/j.jag.2009.11.002

Pekel, J. F., Cottam, A., Gorelick, N., & Belward, A. S. (2016). High-resolution mapping of global surface water and its long-term changes. Nature, 540(7633), 418–422. https://doi.org/10.1038/nature20584

Phan, T. N., Kuch, V., & Lehnert, L. W. (2020). Land cover classification using google earth engine and Random Forest classifier-the role of image composition. Remote Sensing, 12(15). https://doi.org/10.3390/rs1215241c1

PUPR. (2015). Peraturan Menteri Pekerjaan Umum Dan Perumahan Rakyat Republik Indonesia Nomor 28/PRT/M/2015 Tentang Penetapan Garis Sempadan Sungai Dan Garis Sempadan Danau.

Purwanto, A. D., Ibrahim, A., Ulfa, A., Parwati, E., & Supriyono, A. (2022). Pengembangan Model Identifikasi Habitat Bentik Menggunakan Pendekatan Segmentasi Object-Based Image Analysis (OBIA) dan Algoritma Machine Learning (Studi Kasus: Pulau Pari, Kepulauan Seribu). Jurnal Kelautan Nasional, 17(2), 131. https://doi.org/10.15578/jkn.v17i2.10377

Purwanto, A. D., & Setiawan, K. T. (2019). Deteksi Awal Habitat Perairan Laut Dangkal Menggunakan Teknik Optimum Index Factor Pada Citra Spot 7 Dan Landsat 8. Jurnal Kelautan, 4(2), 174–192. https://doi.org/10.31186/jenggano.4.2.174-192

Regasa, M. S., Nones, M., & Adeba, D. (2021). A review on land use and land cover change in ethiopian basins. Journal of Land, 10(6), 1–13. https://doi.org/10.3390/land10060585

Setiawan, K. T., Winarso, G., Ibrahim, A., Purwanto, A. D., & Parsa, I. M. (2022). Comparative Analysis Of Classification Methods For Mapping Shallow Water Habitats Using Spot-7 Satellite Imagery In Nusa Lembongan Island , Bali. 19(01), 11–20.

Trisakti, B., Tjahjaningsih, A., Suwargana, N., Carolita, I., & Mukhoriyah. (2014). Pemanfaatan Penginderaan Jauh Satelit untuk Pemantauan Daerah Tangkapan Air dan Danau (Vol. 7, Issue 1).

Tzotsos, A. (2006). A support vector machine approach for object based image analysis.